

Early presynaptic changes during plasticity in cultured hippocampal neurons

Ipe Ninan¹, Shumin Liu¹, Daniel Rabinowitz² and Ottavio Arancio^{1,*}

¹Taub Institute and Department of Pathology, Columbia University, New York City, NY, USA and ²Department of Statistics, Columbia University, New York City, NY, USA

Long-lasting increase in synaptic strength is thought to underlie learning. An explosion of data has characterized changes in postsynaptic (pstS) AMPA receptor cycling during potentiation. However, changes occurring within the presynaptic (prS) terminal remain largely unknown. We show that appearance of new release sites during potentiation between cultured hippocampal neurons is due to (a) conversion of nonrecycling sites to recycling sites, (b) formation of new releasing sites from areas containing diffuse staining for the prS marker Vesicle-Associated Membrane Protein-2 and (c) budding of new recycling sites from previously existing recycling sites. In addition, potentiation is accompanied by a release probability increase in pre-existing boutons depending upon their individual probability. These prS changes precede and regulate fluorescence increase for pstS GFP-tagged-AMPA-receptor subunit GluR1. These results suggest that potentiation involves early changes in the prS terminal including remodeling and release probability increase of pre-existing synapses.

The EMBO Journal (2006) 25, 4361–4371. doi:10.1038/sj.emboj.7601318; Published online 7 September 2006

Subject Categories: neuroscience

Keywords: cultures; plasticity; synapse; terminal

Introduction

Studies on various hippocampal preparations such as slices, organotypic slices and dissociated cultures have shown evidences in favor of both presynaptic (prS) and postsynaptic (pstS) changes during synaptic plasticity (SP) (Malgaroli and Tsien, 1992; Arancio *et al.*, 1995; Liao *et al.*, 1995; Buchs and Muller, 1996; Ryan *et al.*, 1996; Ma *et al.*, 1999; Toni *et al.*, 1999; Hayashi *et al.*, 2000; Emptage *et al.*, 2003; Humeau *et al.*, 2003; Ninan and Arancio, 2004; Reid *et al.*, 2004). PstS changes have been widely investigated and are thought to be linked to enhanced trafficking of receptors, spine development and pstS currents (Liao *et al.*, 1995; Buchs and Muller, 1996; Toni *et al.*, 1999; Hayashi *et al.*, 2000; Matsuzaki *et al.*, 2004). However, the type of changes occurring in the prS

terminal leading to increased neurotransmitter release is not yet clear.

One of the suggested mechanisms for enhanced transmitter release during SP is recruitment of new release sites (Ma *et al.*, 1999; Toni *et al.*, 1999; Ninan and Arancio, 2004; Reid *et al.*, 2004). However, no data are available on how these new release sites are formed. It has been shown that potentiation is accompanied by a long-lasting increase in cluster number of several prS proteins including synaptophysin (Syp), synapsin I (Syn) and α -synuclein (α Syn), suggesting that a series of coordinate changes occurs at prS level during plasticity (Antonova *et al.*, 2001; Liu *et al.*, 2004; Ninan and Arancio, 2004; Wang *et al.*, 2005). Although it was hypothesized that these clusters correspond to redistribution of prS proteins around pre-existing silent (mute) synapses, it is not clear what these clusters represent in microstructural terms or how they originate. Furthermore, it is not known if there is a relationship between these new release sites and the pstS machinery.

Another cause of the long-lasting transmitter release increase is represented by a release probability increase at pre-existing prS boutons (btns). Limited number of studies on cultured hippocampal neurons suggested enhanced release turnover (Ryan *et al.*, 1996) and readily releasable vesicle pool increase (Stevens and Sullivan, 1998). Earlier electrophysiological studies and statistical analysis suggested high variability in release probability among synapses (Hessler *et al.*, 1993; Rosenmund *et al.*, 1993; Allen and Stevens, 1994; Liu *et al.*, 1999). However, the nature of changes at individual btns in the heterogeneous population of synaptic btns during SP is not clear. Moreover, these studies were inconsistent on whether low-probability or high-probability synapses undergo significant modulation during potentiation. Furthermore, it is not known whether and how such individual release properties affect the pstS machinery.

In the present study, we have used hippocampal neuronal cultures to investigate the nature of both new and pre-existing synapses before and after the tetanus by combining GFP-tagging of the prS marker Vesicle-Associated Membrane Protein (VAMP2-GFP) with staining of release sites using the activity-dependent marker FM4-64. We have found that new synapses arise from (a) conversion of nonrecycling sites, characterized by the presence of VAMP2-GFP puncta, to recycling sites, (b) formation of new releasing sites from areas containing a diffuse staining for VAMP2-GFP and (c) budding of new recycling sites from previously existing recycling sites. We have also found that pre-existing btns undergo increase in release probability during SP depending upon their initial individual release probability. These prS changes precede and regulate AMPA receptors at pstS sites.

Results

Tetanic stimulation of cultured hippocampal neurons (three tetani, 50 Hz, 2 s, 20 s interval, 0 Mg²⁺) modulates sponta-

*Corresponding author. Taub Institute and Department of Pathology, Columbia University, P&S 12-442, 630W, 168th Street, New York City, NY 10032, USA. Tel.: +1 212 342 5527; Fax: +1 212 342 5523; E-mail: oa1@columbia.edu

Received: 2 May 2006; accepted: 8 August 2006; published online: 7 September 2006

neous excitatory pstS currents (sEPSCs), a mix of both miniature excitatory pstS currents (mEPSCs) and spontaneously occurring evoked currents. Tetanus caused an immediate and long-lasting increase of sEPSC frequency ($180.2 \pm 13.6\%$ at 60 min, $n=8$, $F(1,9)=29.6$, $P<0.001$, two-way analysis of variance (ANOVA) with repeated measures, Figure 1A, B and D) and amplitude ($142.7 \pm 5.9\%$ at 60 min, $n=8$, $F(1,9)=23.4$, $P<0.001$, Figure 1A, C and E). Interestingly, at ~ 15 – 20 min we noticed a further increase in sEPSC frequency and curve fitting of the cumulative plotting by Graphpad software suggested at least two distinct phases in the sEPSC frequency increase after the tetanus. The *N*-methyl-D-aspartate (NMDA) receptor antagonist, D-AP5, blocked tetanus-induced potentiation of both sEPSC frequency ($93.9 \pm 7.5\%$, $n=5$, $F(2,13)=16.2$, $P<0.001$, two-way ANOVA with repeated measures, Figure 1A, B and D)

and amplitude ($84.6 \pm 4.9\%$, $n=5$, $F(2,13)=14.3$, $P<0.001$, Figure 1A, C and E), confirming that tetanus-induced SP is NMDA-receptor dependent. Controls without tetanus showed a slight rundown of sEPSC frequency and amplitude presumably due to the whole-cell patch recording over a long duration (Arancio *et al*, 1995).

As previously shown with potentiation in cultures, long-lasting increase of sEPSC frequency and amplitude is dependent upon activation of the nitric oxide-cGMP-dependent protein kinase-calcium/calmodulin-dependent protein kinase II (NO-cGK-CaMKII) pathway (Ninan and Arancio, 2004). The NO-synthase inhibitor L-NMA ($50 \mu\text{M}$), a compound that blocks SP through a direct interaction and inhibition of NO-synthase ($\text{IC}_{50}=6 \mu\text{M}$ in isolated preparations; East and Garthwaite, 1991) blocked tetanus-induced increase in sEPSC frequency ($97.3 \pm 10.7\%$, $n=11$, $F(2,19)=24.6$, $P<0.001$,

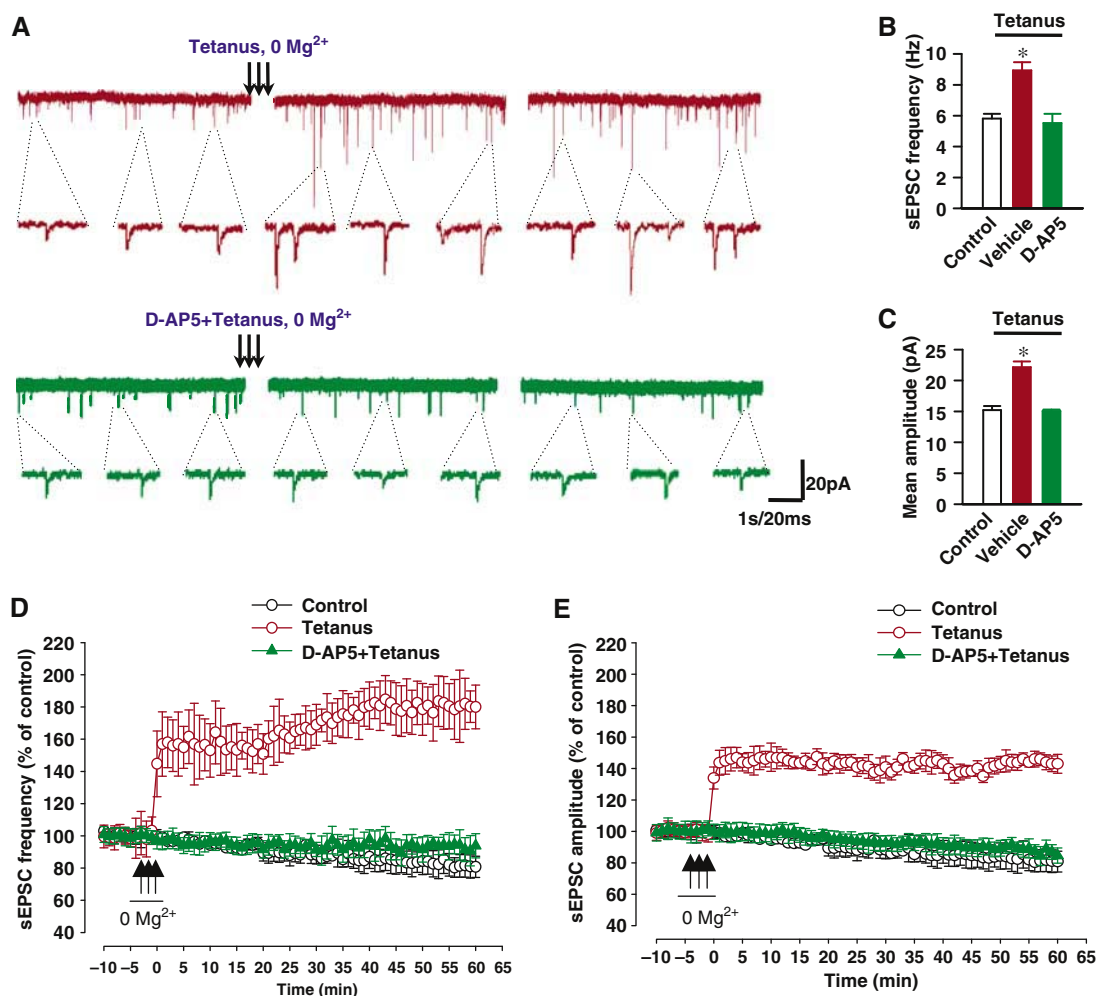


Figure 1 Tetanus in 0 Mg^{2+} increases sEPSC frequency and amplitude in cultured hippocampal neurons. (A) Examples of sEPSCs before and after tetanus. D-AP5 blocked tetanus-induced increase in sEPSCs frequency and amplitude. (B) Average changes in sEPSC frequency in control ($n=3$), tetanus ($n=8$) and D-AP5 + tetanus ($n=5$) groups. D-AP5 reversed the tetanus effect on sEPSC frequency. $*P<0.001$ compared to control group. The mean frequency was 5.8 ± 0.3 , 8.9 ± 0.5 and 5.5 ± 0.6 Hz, for control, tetanus and D-AP5 + tetanus groups, respectively. (C) Average changes in amplitude in control ($n=3$), tetanus ($n=8$) and D-AP5 + tetanus ($n=5$) groups. sEPSC amplitude is increased after tetanus. D-AP5 reversed the tetanus effect on amplitude. $*P<0.001$ compared to control group. The mean amplitudes were 15.2 ± 0.6 , 22.1 ± 0.9 and 15.1 ± 0.2 pA for control, tetanus and D-AP5 + tetanus groups, respectively. (D) Percentage change in sEPSC frequency after tetanus in control ($n=3$), tetanus ($n=8$) and D-AP5 + tetanus ($n=5$) groups. Tetanus produced an immediate and long-lasting increase in sEPSC frequency. D-AP5 blocked tetanus-induced increase in sEPSC frequency (two-way ANOVA with repeated measures). (E) Percentage change in sEPSC amplitude after tetanus in control ($n=3$), tetanus ($n=8$) and D-AP5 + tetanus ($n=5$) groups. Tetanus produced an immediate and long-lasting increase in sEPSC amplitude, which lasted for 60 min. D-AP5 blocked tetanus-induced increase in sEPSC amplitude (two-way ANOVA with repeated measures). Error bars indicate s.e.m. in this and the following graphs.

two-way ANOVA with repeated measures; Supplementary Figure S1A and E) and amplitude ($89.5 \pm 2.4\%$, $n = 11$, $F(2,19) = 25.1$, $P < 0.001$; Supplementary Figure S1B and F). Similarly, KT5823, a specific cGK inhibitor ($K_i = 234$ nM; Kase, 1988) that is also known to block SP suppressed tetanus-induced increase in sEPSC frequency ($86.7 \pm 10.4\%$, $n = 5$, $F(2,12) = 19.3$, $P < 0.001$, two-way ANOVA with repeated measures; Supplementary Figure S1A and E) and amplitude ($85.6 \pm 5.9\%$, $n = 5$, $F(2,12) = 17.5$, $P < 0.001$; Supplementary Figure S1B and F). Finally, KN-93, a membrane-permeable CaMKII inhibitor acting in a competitive fashion against calmodulin (inhibition constant of 0.37 μ M, no significant effects on the catalytic activity of cAMP-dependent protein kinase, Ca^{2+} /phospholipid-dependent protein kinase, myosin light chain kinase and Ca^{2+} -phosphodiesterase; Sumi *et al*, 1991), blocked tetanus-induced increase in sEPSC frequency ($84.5 \pm 5.8\%$, $n = 5$, $F(3,17) = 13.7$, $P < 0.001$, two-way ANOVA with repeated measures; Supplementary Figure S1C and E) and amplitude ($77.9 \pm 2.4\%$, $n = 5$, $F(2,12) = 17.5$, $P < 0.001$, Supplementary Figure S1D and F). KN92, a KN-93 inactive analog, did not affect tetanus-induced increase in frequency ($174.3 \pm 10.4\%$, $n = 5$, Supplementary Figure S1C and E) or amplitude of sEPSCs ($141.9 \pm 5.9\%$, $n = 5$, Supplementary Figure S1D and F). As reported earlier (Ninan and Arancio, 2004), L-NMA, KT5823, KN-93 or KN-92 did not affect basal frequency and amplitude.

Tetani also increased number and fluorescence intensity of prS btms labeled with the cationic styrylpyridinium dye, FM4-64 (10 μ M) (active btm number at 30 min: $191.9 \pm 14.7\%$, $n = 10$, $P < 0.001$, *t*-test, Figure 2A–D). There was no change in prS btm number ($98.5 \pm 5.1\%$, $n = 8$) in control non-tetanzed dishes (Figure 2D). Tetani also increased releasable fluorescence in pre-existing functional prS btms ($209.2 \pm 11.7\%$; 216 btms; $P < 0.001$, *t*-test, Figure 2A–C and E). There was no significant change in releasable fluorescence in control dishes ($99.4 \pm 6.8\%$, 78 btms, Figure 2E). As the cumulative plot of sEPSC frequency suggested the possibility of two distinct SP phases, one immediately and the other one at approximately 15–20 min from the tetanus (Figure 1D), we examined if such phases could be detected in the vesicle cycling. Time-lapse imaging of FM4-64 btms before the tetanus and at 1, 15 and 30 min after it revealed an immediate (1 min) increase in number and fluorescence intensity of prS btms with no further changes at 15 and 30 min after the tetanus suggesting that the slight increase in sEPSC frequency observed at 15–20 after the tetanus is not due to changes in vesicle cycling (Supplementary Figure S2).

Tetanus-induced changes in the prS release apparatus were NMDA receptor-dependent. D-AP5 (40 μ M) blocked increase in number ($97.4 \pm 4.3\%$, $n = 9$, $F(2,24) = 29.6$, $P < 0.001$, one-way ANOVA followed by LSD; Figure 2A, B and D) and releasable fluorescence ($96.4 \pm 3.5\%$, 56 btms, $F(2,348) = 42.3$, $P < 0.001$; Figure 2A, B and E) of the prS btms. Tetanus increased only prS btm number but not releasable fluorescence in pre-existing functional synapses when staining was performed using high K^+ solution instead of electrical stimulation confirming that detection of fluorescence intensity increase is not feasible under intense loading conditions (Ma *et al*, 1999; Ninan and Arancio, 2004) (Supplementary Figure S3).

Similar to long-lasting increase of sEPSC frequency and amplitude, tetanus-induced prS changes in functionally active

btm number and releasable fluorescence involve the NO-cGK-CaMKII pathway. L-NMA (50 μ M) or KT5823 (2 μ M) blocked tetanus-induced increase in functionally active btm number ($92.4 \pm 3.1\%$, $n = 12$, $F(2,27) = 37.9$, $P < 0.001$, one-way ANOVA followed by LSD and $97.9 \pm 2.6\%$, $n = 10$, $F(2,25) = 32.4$, $P < 0.001$; Figure 2F). Similarly, we observed complete blockade of tetanus-induced increase in releasable fluorescence by L-NMA or KT5823 ($98.6 \pm 5.2\%$, $n = 69$, $F(2,361) = 31.2$, $P < 0.001$, one-way ANOVA followed by LSD and $97.7 \pm 6.5\%$, $n = 71$, $F(2,363) = 33.7$, $P < 0.001$; Figure 2G). KN-93 (5 μ M), but not KN-92, blocked tetanus-induced increase in functional btm number ($96.7 \pm 4.4\%$, $n = 10$ and $199.9 \pm 13.7\%$, $n = 7$, for KN-93 and KN-92 groups, respectively, $F(3,31) = 28.1$, $P < 0.001$, one-way ANOVA followed by LSD; Figure 2H) and releasable fluorescence ($95.9 \pm 7\%$, $n = 77$ and $202.4 \pm 23.2\%$, $n = 29$, for KN-93 and KN-92 groups, respectively; $F(3,397) = 24.1$, $P < 0.001$, one-way ANOVA followed by LSD; Figure 2I). These findings confirm previous experiments showing an NO/cGK/CaMKII pathway-dependent increase in active btm number during SP (Ninan and Arancio, 2004). Most importantly, with the use of electrical stimulation, these experiments show the presence of NO/cGK/CaMKII-dependent increase in fluorescence of pre-existing active btms.

What is the origin of the new functional release sites? The increase in functional synapse number following tetanus suggests the occurrence of microstructural changes leading to the formation of a mature release apparatus. To provide proof in favor of such changes, we transfected cultured hippocampal neurons with plasmid for the prS marker VAMP2 labeled with GFP. VAMP2-GFP fusion protein incorporates into synaptic vesicles. As reported earlier (Ahmari *et al*, 2000; Sampo *et al*, 2003), most of VAMP2-GFP fluorescence appeared punctate (Figure 3A and B) along the axon in 10-day-old cultures. The remaining fluorescence appeared relatively diffuse (Figure 3A and C). Consistent with these studies, soma and dendrites showed lighter and diffused fluorescence. The size of VAMP2-GFP puncta was between 0.5 and -1.5 μ m. When we examined recycling characteristics of VAMP2-GFP puncta by loading with FM4-64, we found that only $59.5 \pm 2.5\%$ (22 dishes) of VAMP2-GFP puncta were functionally active btms (as shown by the conversion of green VAMP2-GFP puncta to yellow puncta after FM staining). Comparison of VAMP2-GFP-expressing neurites with control GFP-expressing neurites revealed no significant difference in functional btm number between VAMP2-GFP-transfected neurites and control neurites (4.3 ± 0.4 btms/ 30 μ m, $n = 28$ and 4.4 ± 0.6 btms/ 30 μ m, $n = 31$, respectively). Similarly, there was no significant difference in btm intensity at VAMP2-GFP-transfected and control neurites (37.8 ± 2.7 arbitrary units (au), $n = 51$ and 37.5 ± 2.9 au, $n = 59$, respectively). Tetanus increased the number of VAMP2-GFP puncta colocalized with recycling btms ($99.2 \pm 6\%$ of total VAMP2-GFP puncta, $n = 15$), producing a $187.8 \pm 4.7\%$ increase in recycling VAMP2-GFP puncta number (compare yellow puncta before and after tetanus in Figure 3D). This increase was due to (a) green puncta that were not FM stained by the first staining performed before the tetanus but were stained (appeared yellow) by the second staining performed after the tetanus (Figure 3E and H), (b) fusion of diffused VAMP2-GFP with no FM staining before the tetanus to become a recycling btm (appeared yellow after the tetanus) (Figure 3F

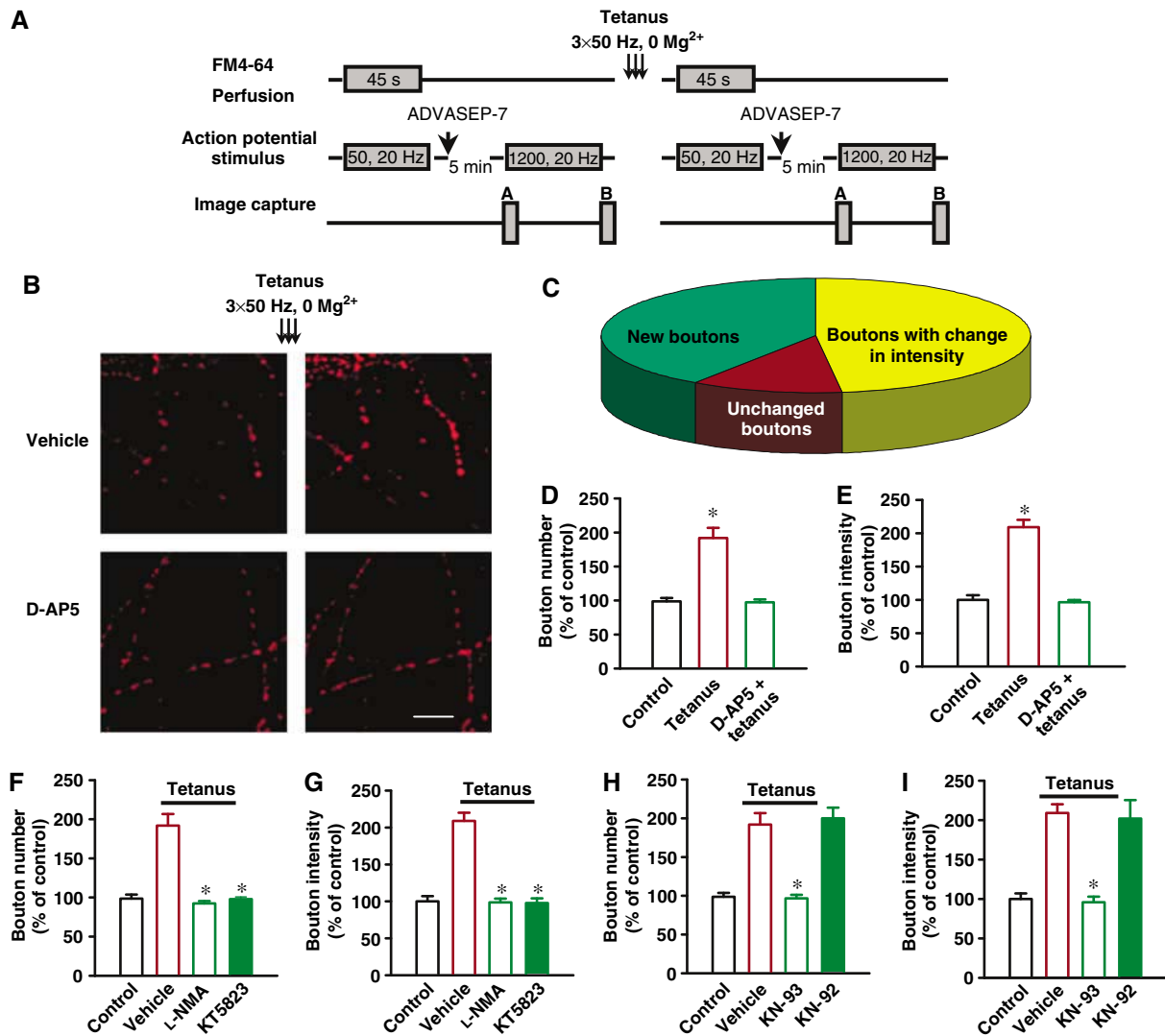


Figure 2 Tetanus in 0 Mg²⁺ increases functional prS btm number and releasable fluorescence in cultured hippocampal neurons. (A) Experimental protocol for staining, destaining and tetanus application using electrical stimulation. ADVASEP-7 (1 mM), an anionic cyclodextrin complexing agent with higher affinity for the dye than the plasma membrane was introduced in the washing bath solution for enhanced removal of the dye from the external medium to reduce background staining. (B) Examples of activity-dependent FM4-64 staining before and after tetanus. Tetanus in 0 Mg²⁺ increased prS btm number and releasable fluorescence intensity in pre-existing prS btms. D-AP5 (40 μM) blocked tetanus-induced plasticity. Scale bar 10 μm. (C) A pie chart representing percentage of new btms, btms that underwent changes in fluorescence intensity and unchanged btms, after tetanus (*n* = 5). (D) Percentage increases in number of functional prS btms 30 min after tetanus. D-AP5 (40 μM) completely blocked tetanus-induced increase in recycling btm number (one-way ANOVA followed by LSD). **P* < 0.001 compared to control group. (E) Percentage increase in releasable fluorescence of pre-existing functional prS btms 30 min after tetanus. D-AP5 (40 μM) blocked tetanus-induced releasable fluorescence increase. **P* < 0.001 compared to control group. NO synthase inhibitor, L-NMA (50 μM) and cGK inhibitor, KT5823 (2 μM) blocked tetanus-induced increase in prS btm number (F) and releasable fluorescence (G) in pre-existing prS btms. CaMKII inhibitor, KN-93 (5 μM) but not its inactive analog, KN-92 (5 μM) blocked tetanus-induced increase in prS btm number (H) and releasable fluorescence (I) in pre-existing prS btms (one-way ANOVA followed by LSD). **P* < 0.001 compared to tetanus.

and H) and (c) budding of new recycling btms from pre-existing recycling btms (Figure 3G and H). Although most of the nonrecycling green puncta that underwent conversion into recycling puncta following tetanus did not show a change in fluorescence, a minor number of these converted puncta showed a VAMP2-GFP staining intensity increase associated with a decrease in diffused GFP intensity at either sides of the btm suggesting mobilization of VAMP2 to synaptic sites from nonsynaptic sites. We also examined total area and average intensity of green fluorescence per 30 μm of transfected axons. There was no significant difference in either total area (57.4 ± 14.6 and 53.4 ± 12.2 pixel², respectively,

n = 7) or average intensity (34.8 ± 3.7 au, *n* = 7 and 42.9 ± 4 au, *n* = 6, respectively) of green fluorescence before and after tetanus. However, adjusting the threshold to exclude low fluorescence intensity areas showed 23.6% decrease in total area of green fluorescence after tetanus suggesting mobilization of VAMP2 to synaptic sites. We also tested whether inhibitors of NO synthase, cGK or CaMKII could block tetanus-induced increase in number of FM4-64 positive and therefore recycling VAMP2-GFP puncta. Increase in FM4-64-positive VAMP2-GFP puncta number was blocked by L-NMA (4.8 ± 0.3 and 5 ± 0.4/30 μm, respectively before and after tetanus, *n* = 12), KT5823 (4.7 ± 0.4 and 4.5 ± 0.5/30 μm,

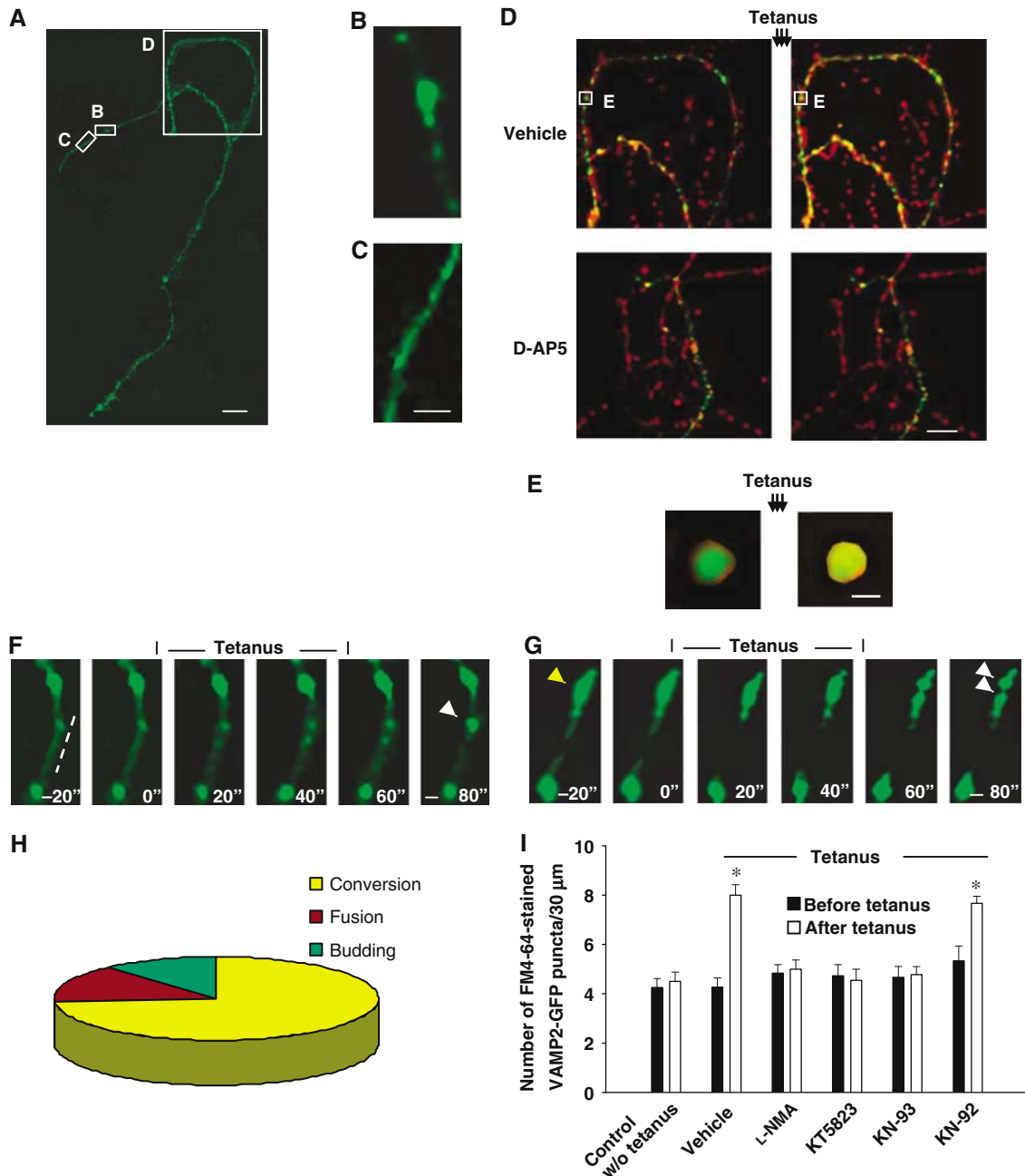


Figure 3 Tetanus induces prS remodeling in cultured hippocampal neurons to enhance transmitter release. (A) Example of an axon expressing VAMP2-GFP fusion protein. Scale bar 10 μ m. (B, C) Examples of punctated (B) and diffused (C) fluorescence from the axon expressing VAMP2-GFP fusion protein shown in (A). Scale bar 2 μ m. (D) Examples of activity-dependent staining of FM4-64 before and after tetanus in cultures transfected with VAMP2-GFP. Tetanus increased number of yellow puncta (FM4-64 staining in VAMP2-GFP expressing axon) as well as red puncta (FM4-64 staining in nontransfected axons). Tetanus also increased releasable fluorescence in btns from both transfected and nontransfected axons. D-AP5 (40 μ M) blocked tetanus-induced increase in btn number and releasable fluorescence (one-way ANOVA followed by LSD). Scale bar 10 μ m. (E) Insets show a VAMP2-GFP punctum that becomes recycling after tetanus. Scale bar 1 μ m. (F) An example of fusion of diffused VAMP2-GFP to become a recycling btn. The dashed line shows the diffused fluorescence. The arrow shows the new btn. Scale bar 1 μ m. (G) An example of budding of new VAMP2-GFP btns from a pre-existing VAMP2-GFP btn. The yellow arrow shows the original btn whereas the white arrow shows the new btns. Scale bar 1 μ m. (H) A pie chart representing percentage contribution of (1) conversion of nonrecycling pre-existing btns to recycling btns (74%), (2) fusion of nonsynaptic VAMP2-GFP (14.3%) and (3) budding from pre-existing recycling btns (11.7%) in tetanus-induced increase in VAMP2-GFP recycling btn number calculated from 15 samples. (I) Number of FM4-64 stained btns per 30 μ m of VAMP2-GFP expressing axons in control (8), tetanus (15), L-NMA paired with tetanus (12), KT5823 paired with tetanus (11), KN-93 paired with tetanus (8) and KN-92 paired with tetanus (8) groups before (filled bar) and 30 min after (empty bar) the tetanus. The empty bar in the control group represents parallel measurement of number of FM4-64 positive VAMP2-GFP puncta at 30 min without tetanus. L-NMA, KT5823, KN-93 but not KN-92 blocked tetanus-induced increase in FM4-64 recycling btn number. In L-NMA, KT5823, KN-93 but not KN-92 groups, we neither observed fusion of nonsynaptic VAMP2-GFP nor budding from recycling VAMP2-GFP btns. * P < 0.001 compared to pretetanus value.

respectively before and after tetanus, $n = 11$) and KN-93 (4.7 ± 0.4 and $4.8 \pm 0.3/30 \mu\text{m}$, respectively before and after tetanus, $n = 8$; Figure 3I).

Earlier studies have demonstrated a prS btn number increase after cAMP signaling activation in cultured hippocampal neurons (Ma *et al*, 1999). In preliminary studies, we found that elevating cAMP levels by perfusion of forskolin or IBMX produces similar results as our tetanus (Supplementary Results and Supplementary Figure S4). The occlusion of the effect of forskolin and IBMX on btn number and fluorescence intensity by tetanus suggests that these two SP processes share similar mechanisms (Supplementary Results and Supplementary Figure S4).

Earlier studies have suggested an inverse relationship between the initial release probability of a synapse and its ability to undergo plasticity changes (Hessler *et al*, 1993; Bi and Poo, 1998). However, technical difficulties prevented a direct analysis of release probability at the level of individual btms. As we found high variability of releasable fluorescence among individual prS btms when stained with 50 action potentials (Ninan *et al*, 2005) at 20 Hz corresponding to btms with different release probabilities, we wanted to examine whether initial release probability determines ability of individual prS btms to undergo potentiation. Calculation of releasable fluorescence of a single vesicle was based on the assumption that a single action potential causes release of one vesicle (Supplementary data). Synaptic vesicles were stained by perfusing FM4-64 (10 μM) for 10 s and eliciting one action potential. Releasable fluorescence of a single vesicle was calculated after destaining with 1200 action potentials at 20 Hz (Figure 4A and B). As described, probability of individual synapses was calculated by using the formula $\text{Pr} = \text{releasable fluorescence of a btm} / \text{number of action potentials} \times \text{releasable fluorescence of a single vesicle}$ (Slutsky *et al*, 2004). Measurement of release probabilities of 216 active btms ($n = 5$ dishes) showed three categories of btms based on their initial probabilities: low ($\text{Pr} = 0.01\text{--}0.0999$, $n = 114$), medium ($\text{Pr} = 0.1\text{--}0.1999$, $n = 70$) and high-probability btms ($\text{Pr} > 0.2000$, $n = 32$) (Supplementary Figure S5A, B and C). Tetanus increased Pr values for the low (median 0.0727 and 0.1846 before and after tetanus) and medium (median 0.1451 and 0.1811 before and after tetanus)-probability populations ($P < 0.001$, Wilcoxon's matched pairs test; Supplementary Figure S5C). The high-probability population did not undergo any significant change (median 0.2129 and 0.1892 before and after tetanus) in release probability. These results are consistent with the notion of an inverse relationship between initial release probability of a synapse and its ability to undergo SP changes (Hessler *et al*, 1993; Bi and Poo, 1998). Most importantly, they extend findings from synapses made of a population of heterogeneous btms to the level of individual btms. Thus, the present study suggests that tetanus increases number of vesicles available for release and thereby enhances release. Interestingly, we have observed that post-tetanus Pr values are identical in all the three populations suggesting a ceiling effect on number of vesicles available for release under our experimental conditions. L-NMA (post-tetanic median values 0.0717 and 0.1286, respectively, for low and medium-probability btms), KT5823 (post-tetanic median values 0.0786 and 0.1458, respectively, for low and medium-probability btms) and KN-93 (post-tetanic median values 0.0712 and 0.1522, respectively, for low and medium-

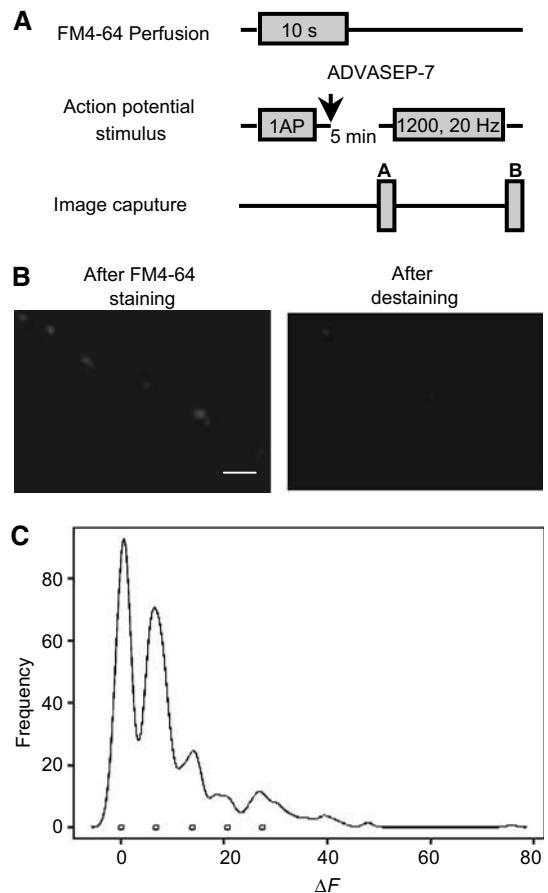


Figure 4 (A) Experimental protocol for the estimation of single vesicle fluorescence. Synaptic vesicles were loaded with FM4-64 by perfusing the neurons with bath solution containing FM4-64 for 10 s, and eliciting 1 action potential. (B) Examples of activity-dependent FM4-64 staining before and after destaining. Scale bar 5 μm . (C) A histogram of intensities of 546 active btms stained with 1 action potential. The first peak corresponds to btms showing non-specific staining whereas the second peak represents btms that released one vesicle.

probability btms) blocked tetanus-induced increase of release probability in low and medium-probability btms (Supplementary Figure S5D–F and G).

Previous studies have shown that SP is associated with pstS changes such as increase in AMPA receptors GluR1 subunit at synaptic sites (Shi *et al*, 1999; Lu *et al*, 2001; Pickard *et al*, 2001). Thus, we examined whether there was a relationship between prS and pstS changes at individual synapses. To follow pstS changes, neurons were transfected with GluR1-GFP plasmid. Similar to a previous study (Shi *et al*, 1999), the recombinant protein was distributed throughout the dendrite and the soma with a punctated pattern (Figure 5A). In the same study, GluR1 protein was colocalized with endogenous GluR2 and Syn, and homomeric recombinant receptors were functionally delivered to the surface. We found relatively more intense GluR1-GFP puncta at locations apposed to active prS btms that were stained with FM4-64. We did not see any difference in number or intensity of FM4-64 btms apposing the dendrites of GluR1-GFP-expressing cells compared to nonexpressing cells. Next, we examined whether tetanus affected fluorescence intensity of GluR1-GFP puncta at releasing sites. Time-lapse imaging revealed a GluR1-GFP intensity increase at releasing sites

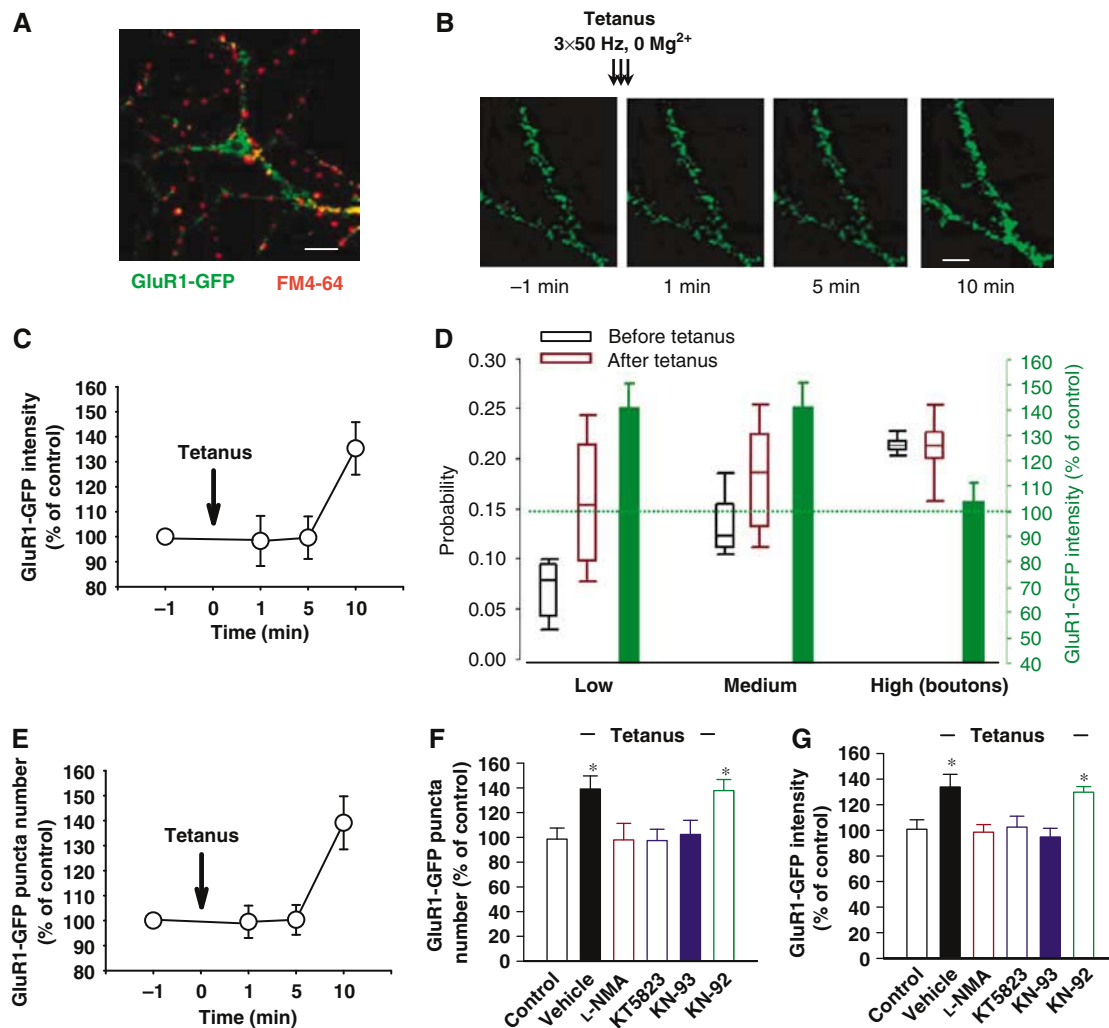


Figure 5 Tetanus produces a delayed increase in GluR1-GFP fluorescence intensity and puncta number in cultured hippocampal neurons. (A) Example of a GluR1-GFP fusion protein expressing culture stained with FM4-64. GluR1-GFP was distributed both in soma and dendrites. FM4-64 staining demonstrated relatively more intense GluR1-GFP fluorescence opposed to prS btms. Scale bar 10 μ m. (B) Examples of GluR1-GFP-expressing dendrites at 1 min before the tetanus and 1, 5 and 10 min after it. A clear increase of GluR1-GFP fluorescence intensity and puncta number was visible at 10 min but not at 1 or 5 min after the tetanus. Scale bar 3 μ m. (C) Time course of the percentage increase in GluR1-GFP fluorescence intensity before and after tetanus. (D) Tetanus-induced increase in release probability affects GluR1-GFP fluorescence at individual synapses. Probability increase at low ($n=49$) and medium ($n=34$)-probability sites was associated with a GluR1-GFP fluorescence increase ($P<0.05$, t -test). However, pstS sites opposite to high-probability sites ($n=23$) did not undergo any change in GluR1-GFP fluorescence after tetanus. Error bars above and below the empty box indicate the 90th and 10th percentiles whereas the error bars on the green box indicate s.e.m. (E) Time course of the percentage increase in GluR1-GFP puncta number before and after tetanus. (F) Percentage changes in GluR1-GFP puncta number in control ($n=5$), tetanus ($n=8$), L-NMA paired with tetanus ($n=4$), KT5823 paired with tetanus ($n=4$), KN-93 paired with tetanus ($n=5$) and KN-92 paired with tetanus ($n=3$) groups. L-NMA, KT5823 and KN-93 but not KN-92 reversed the tetanus effect on GluR1-GFP puncta number. $*P<0.05$ compared to control group. (G) Percentage changes in fluorescence intensity of GluR1-GFP puncta in control ($n=41$), tetanus ($n=106$), L-NMA paired with tetanus ($n=43$), KT5823 paired with tetanus ($n=36$), KN-93 paired with tetanus ($n=37$) and KN-92 paired with tetanus ($n=23$) groups. L-NMA, KT5823 and KN-93 but not KN-92 reversed the effect of tetanus on GluR1-GFP puncta fluorescence intensity. $*P<0.05$ compared to control.

($135.3 \pm 10.5\%$, $n=30$, $P<0.01$, t -test) 10 min after the tetanus whereas there was no GluR1-GFP intensity increase at 1 ($98.3 \pm 9.9\%$, $n=30$) or 5 min ($99.6 \pm 8.5\%$, $n=26$; Figure 5B and C). This finding is consistent with experiments in organotypic cultures demonstrating insertion of the GluR1 subunit at 15–20 min after tetanus (Shi *et al*, 1999). Similar to the studies shown in Supplementary Figure S5, we found three release probability kinds of prS btms: low, medium and high probability. Fluorescence measurements of GluR1 puncta opposite to prS btms revealed an interesting relationship between release probability and changes in GluR1-GFP fluorescence. Release probability increase at low (median

0.0785 and 0.1599 before and after tetanus) and medium (median 0.1221 and 0.1846 before and after tetanus)-probability sites was associated with a GluR1-GFP fluorescence intensity increase at 30 min after the tetanus ($141.5 \pm 12.9\%$, $n=49$, and $142.9 \pm 13.2\%$, $n=34$, respectively, $P<0.05$, t -test, Figure 5D). However, GluR1-GFP fluorescence at sites opposite to high-probability sites (median 0.2151 and 0.2180 before and after tetanus) did not change after tetanus ($103.9 \pm 7.4\%$, $n=23$; Figure 5D). These results suggest an increase in GluR1-GFP fluorescence intensity at synaptic sites dependent upon release probability increase. Furthermore, analyses of the average basal fluorescence intensity for

GluR1-GFP revealed lower fluorescence (54.4 ± 6.7 au, $n = 23$) at sites opposite to high-probability release sites compared to sites opposite to low-probability sites (69.4 ± 5.5 au, $n = 49$) and sites opposite to medium-probability sites (68.4 ± 7.3 au, $n = 34$) suggesting a possible compensatory decrease in GluR1 expression at high-probability sites.

Next, we studied if conversion of mute synapses affected pstS GluR1 fluorescence. We analyzed GluR1 fluorescence opposite to the newly converted btns ($n = 26$) by retrospectively measuring GluR1 fluorescence at sites that were not stained with FM4-64 before the tetanus. We found $138.4 \pm 11.4\%$ increase ($P < 0.01$, t -test) in GluR1 intensity at sites opposite to the newly converted btns 10 min after the tetanus. Consistent with the earlier reports that glutamate increased GluR1 immunoreactive puncta number (Antonova *et al*, 2001), we found a GluR1-GFP puncta number increase 10 min after tetanus but not at 1 or 5 min (10 min: $139.1 \pm 10.6\%$, $n = 8$, $P < 0.05$, t -test; 1 min: $99.5 \pm 6.5\%$, $n = 8$; 5 min: $100.3 \pm 5.7\%$, $n = 8$; Figure 5E). Similar to tetanus-induced changes in prS btns, L-NMA, KT5823 or KN-93 completely blocked tetanus-induced increase in GluR1-GFP puncta

number ($98 \pm 13.3\%$, $n = 4$; $97.5 \pm 9.1\%$, $n = 4$; $102.4 \pm 11.4\%$, $n = 5$; Figure 5F) and fluorescence at synaptic sites ($98.5 \pm 5.9\%$, $n = 43$, $102.5 \pm 8.5\%$, $n = 36$ and $94.8 \pm 6.8\%$, $n = 37$, respectively; Figure 5G). Thus, these findings strongly support the hypothesis that tetanus-induced prS changes in cultured hippocampal neurons precede and regulate postsynaptic changes at the level of the GluR1 subunit.

We finally determined whether probability conditions influence tetanus-induced SP in cultured hippocampal neurons both at the prS and pstS level. Ca^{2+}/Mg^{2+} ratio increase from 2:2 to 3.5:0.5 (Figure 6A) increased release probability in both low (median 0.0698 and 0.1802 before and after changing calcium/magnesium ratio, $n = 47$) and medium (median 0.1308 and 0.2093 before and after changing Ca^{2+}/Mg^{2+} ratio, $n = 35$)-probability btns (Figure 6B and C), augmented prS btn number ($172.9 \pm 14\%$, $n = 8$, $P < 0.05$) (Figure 6B and D), and increased GluR1-GFP fluorescence apposed to low and medium-probability btns ($140.8 \pm 6.9\%$, $n = 47$ and $143.7 \pm 7.8\%$, $n = 35$, respectively, $P < 0.01$; Figure 6B and C). Furthermore, release probability increase enhanced GluR1-GFP puncta number ($131.6 \pm 6.6\%$, $n = 5$,

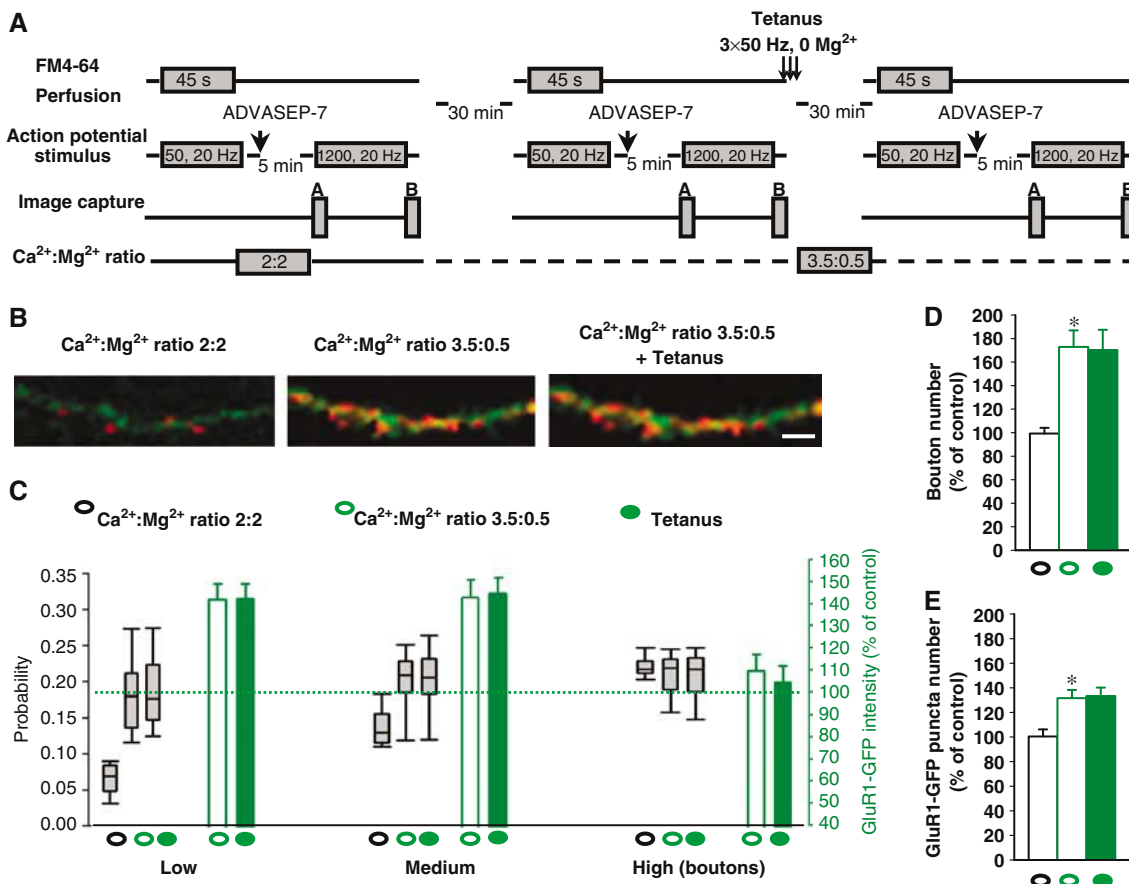


Figure 6 Release probability increase enhances GluR1-GFP fluorescence and puncta number in cultured hippocampal neurons and occludes tetanus-induced plasticity. (A) Experimental protocol under different Ca^{2+}/Mg^{2+} ratio conditions. (B) Examples of FM4-64 staining in GluR1-GFP-expressing neurites under normal Ca^{2+}/Mg^{2+} ratio (2:2), high Ca^{2+}/Mg^{2+} ratio (3.5:0.5) and after the tetanus in high Ca^{2+}/Mg^{2+} ratio (3.5:0.5). Scale bar 3 μm . (C) Increase in Ca^{2+}/Mg^{2+} ratio enhanced release probability in both low ($n = 47$) and medium ($n = 35$)-probability btns and GluR1-GFP fluorescence apposed to low and medium-probability btns. High-probability btns did not show any increase in release probability. Similarly, there was no increase in GluR1-GFP fluorescence apposed to high-probability btns. There was no further increase of probability in prS btns or GluR1-GFP fluorescence when the same cultures bathed in high-probability release solution received a tetanus. Error bars above and below the grey empty box indicate the 90th and 10th percentiles whereas the error bars on both empty and filled green boxes indicate s.e.m. (D) Ca^{2+}/Mg^{2+} ratio increase resulted in potentiation of prS btn number with no further increase in btn number when the same cultures bathed in high-probability release solution received a tetanus in 0 Mg^{2+} . * $P < 0.001$ compared to control group. (E) Ca^{2+}/Mg^{2+} ratio increase resulted in potentiation of GluR1-GFP puncta number with no further increase in GluR1-GFP puncta number when the same cultures bathed in high-probability release solution received a tetanus in 0 Mg^{2+} . * $P < 0.05$ compared to control group.

$P < 0.05$, *t*-test, Figure 6B and E). High-probability btms did not show any further increase (median 0.2180 and 0.2209 before and after changing $\text{Ca}^{2+}/\text{Mg}^{2+}$ ratio, $n = 19$) in release probability (Figure 6C). Similarly, there was no increase in GluR1-GFP fluorescence apposed to high-probability btms ($109.7 \pm 7.3\%$, $n = 19$). Next, we applied tetanus to determine whether it is possible to induce potentiation under high-probability conditions. There was no further release probability increase in prS btms (median 0.1773, 0.2064 and 0.2180, respectively, for btms that were classified as low, medium and high probability before changing the $\text{Ca}^{2+}/\text{Mg}^{2+}$ ratio; Figure 6B and C), btn number ($170.3 \pm 17.1\%$, $n = 8$, Figure 6B and D) or GluR1-GFP fluorescence ($141 \pm 6.5\%$, $n = 47$ and $145.4 \pm 7.2\%$, $n = 35$ and $104.9 \pm 7.2\%$, $n = 19$, respectively, for low, medium and high-probability release btms; Figure 6B and C). Similarly, tetanus did not further increase GluR1-GFP puncta number ($133.4 \pm 6.8\%$, $n = 5$; Figure 6B and E) under high-probability conditions. These results suggest that high-probability conditions occlude tetanus-induced SP in cultured hippocampal neurons and further confirm that transmitter release at single synapses regulates the extend of pStS activation.

Discussion

Our results demonstrate that potentiation in cultured hippocampal neurons is accompanied by a transmitter release increase through appearance of new prS release sites and release probability increase at pre-existing functional synapses in an NMDA receptor-dependent manner. These findings are in agreement with previous reports showing that glutamate increases functional prS release site number (Ninan and Arancio, 2004). However, in the same study, glutamate did not affect releasable fluorescence intensity in pre-existing prS btms, probably because of maximum staining evoked by the high K^+ loading solution used in that experimental paradigm (Ma *et al*, 1999; Ninan and Arancio, 2004). In the present study to avoid maximum staining, we have used a different staining protocol in which electrical stimulation has been shown to selectively empty only readily releasable vesicle pool (Rosenmund and Stevens, 1996; Dobrunz and Stevens, 1997; Murthy and Stevens, 1998). Our results also agree with earlier reports showing an enhanced transmitter turnover using a different tetanus protocol (50 Hz, 30 s) (Ryan *et al*, 1996). However, this protocol failed to increase btn number in the presence of Mg^{2+} . It is plausible that removal of NMDA receptor blockade by 0Mg^{2+} solution during the tetanus in our experiments might activate conversion of mute synapses (Antonova *et al*, 2001; Ninan and Arancio, 2004). Thus, with our new experimental conditions, we have been able to provide a comprehensive analysis of the kinds of changes occurring during SP at synaptic btms.

Previous studies showed increase in functional prS btn number immediately after SP induction (Ninan and Arancio, 2004). However, these studies did not follow the behavior of these new sites over time and thus, did not include a retrospective analysis of their behavior before SP. Increase in cluster number for prS proteins Syp, Syn and αSyn was documented during potentiation (Antonova *et al*, 2001; Liu *et al*, 2004). However, it was not clear what these clusters represent in microstructural terms or how they originate. By transfection of cultured hippocampal neurons with VAMP2-

GFP and subsequent FM staining, we have been able to show that these new functional release sites are either at their nascent state before the tetanus or formed from prS rearrangement to become releasing sites after the tetanus. The former are very similar to mature sites except that they have zero release probability. The latter are immature release sites and need release apparatus rearrangement, including (i) fusion of diffuse staining for VAMP2-GFP to become functionally active release sites and (ii) budding of new release sites from already existing functional release sites. These findings are consistent with the clustering of previously synthesized prS proteins Syn, Syp and αSyn , as well as pStS GluR1 during plasticity (Carroll *et al*, 1999; Lissin *et al*, 1999; Shi *et al*, 1999; Antonova *et al*, 2001; Liu *et al*, 2004; Wang *et al*, 2005). Interestingly, the percentage increase in 'budding' in prS btms following tetanus was similar to the perforated synapse number increase during SP reported in other studies following induction of plasticity (Neuhoff *et al*, 1999; Toni *et al*, 2001; Stewart *et al*, 2005).

An earlier study on VAMP2-GFP-expressing hippocampal cells showed that vesicular packets containing cytoplasmic and membrane-associated protein precursors for synaptic vesicles are transported along axons and get stabilized at synaptic sites (Ahmari *et al*, 2000). Thus, our results suggest that tetanus accelerates mobilization of prS vesicular precursors to enhance transmitter release.

Consistent with the notion that release probability is nonuniform among synapses (Hessler *et al*, 1993; Rosenmund *et al*, 1993; Allen and Stevens, 1994; Liu *et al*, 1999), our study show a population of FM4-64 puncta with highly variable releasable fluorescence. There were inconsistent reports on whether low or high-probability synapses undergo significant modulation during potentiation (Hessler *et al*, 1993; Rosenmund *et al*, 1993; Bi and Poo, 1998). Thus, we classified the prS btms into low, medium and high-probability sites based on their initial release probability and then studied them individually. Tetanus potentiated release probability in low and medium-probability sites but not in high-probability sites. These results are consistent with the notion that SP at individual synapses is inversely related to the initial release probability at those synapses. In other words, our results suggest that low-probability sites offer a greater window for potentiation than high-probability sites. This finding agrees with a previous study on LTP in the CA1 pyramidal neurons showing a release probability increase only at synapses with low baseline probability (Palmer *et al*, 2004). Interestingly, the maximum release probability after tetanus in low and medium-probability btms was similar to the probability at high-probability btms, which did not undergo any significant probability increase after tetanus. This suggests that under our experimental conditions, there is a ceiling effect on the maximum release probability, which suggests that there is no increase in available pool of vesicles but enhanced transmitter turnover in the available pool of vesicles after the tetanus (Ryan *et al*, 1996).

Consistent with the results from FM4-64 staining studies, tetanus produced an immediate and long-lasting increase in sEPSC frequency and amplitude in an NMDA receptor-dependent fashion. As there is no change in GluR1-GFP fluorescence at synaptic sites immediately after tetanus, possible reasons for the immediate sEPSC amplitude increase might be either prS (Choi *et al*, 2000; Renger *et al*, 2001) or an

increase in AMPA receptor conductance (Benke *et al*, 1998; Palmer *et al*, 2004). A possible relationship between prS modulation and the increased sEPSC amplitude depends on quanta released number and quantal size. Release site number as well as release probability influence the number of quanta released and tetanus increased both release site number and probability in pre-existing synapses strongly supporting the hypothesis that EPSC amplitude increase is due to prS modulation. However, it is not possible to exclude that pstS changes such as increased AMPA receptor conductance or changes in the AMPA receptor subunit distribution between the intracellular- and the surface-compartment (our technique does not distinguish between the two compartments) contribute to immediate sEPSC amplitude increase. The late AMPA receptor mobilization to synaptic sites as seen in our experiments and on tetanized organotypic slice experiments (Shi *et al*, 1999) might contribute to the maintenance of SP. Interestingly, we found two distinct phases during sEPSC frequency increase after the tetanus suggesting that two distinct mechanisms underlie SP. Given that the FM studies revealed no further changes in the increase in btn number and release probability after the initial changes, we infer that the observed biphasic increase in sEPSC frequency after the tetanus is not due to prS changes. Thus, the delayed increase in GluR1 activity might underlie the second SP phase.

Earlier studies using expression of the GluR1-GFP fusion protein in organotypic slices showed that the distribution of the GluR1-GFP fusion protein mimics intracellular endogenous GluR1 distribution (Shi *et al*, 1999; Hayashi *et al*, 2000). In the present study, we have confirmed this finding at synaptic sites of cultured hippocampal neurons. In addition, we have observed a GluR1-GFP fluorescence intensity increase at synaptic sites where there was a release probability increase and appearance of new GluR1 puncta dependent upon the retrograde messenger cascade activation. There was no GluR1-GFP fluorescence increase at high-probability synapses, which also remained unmodified. Our results under low and high-probability conditions show that the tetanus-induced increase in GluR1-GFP fluorescence at individual synapses depends on release probability increase at those synapses suggesting that the extent of prS potentiation determines the extent of pstS AMPA receptor activation. Thus, these results together with the demonstration that the GluR1-GFP intensity increase happens at 10 min after tetanus but not at 1 min after tetanus, suggest that tetanus-induced long-lasting potentiation in cultured hippocampal neurons primarily involves immediate prS changes that in turn modulate pstS machinery. As previous studies have shown membrane insertion of AMPA receptors during SP in both cultured

hippocampal neurons (Lu *et al*, 2001; Pickard *et al*, 2001) and organotypic slice cultures (Shi *et al*, 1999), we infer that the GluR1-GFP increase at synaptic sites observed in our studies involves plasma membrane GluR1 insertion. Moreover, there was lower basal GluR1 fluorescence at high-probability sites reflecting compensatory phenomena at individual synapses. Such compensatory mechanisms have been observed in cultured hippocampal neurons in which the average size of synaptic currents and of responses to focal glutamate application varied four-fold across different cells, decreasing markedly with increasingly dense synaptic innervation (Liu and Tsien, 1995). In other words, our data suggest that an ongoing cross-talk between prS and pstS sites controls pstS activation during SP. Further, these data suggest how precisely release probability regulates synaptic strengthening at individual synapses.

Materials and methods

Cell cultures and transfection

Primary cultures were prepared from 1–2-day-old B6SJL/J mouse pups as described earlier (Arancio *et al*, 1995; Ninan and Arancio, 2004). Neurons were transfected on day 1 by electroporation using Nucleofector 1 (Amaxa Biosystems; Supplementary Materials and methods).

Electrophysiology

The glass coverslip containing 10–15-day-old hippocampal neurons was transferred to the recording chamber. Neurons were held under ruptured whole-cell voltage clamp throughout the experiment; sEPSCs were measured as described (Arancio *et al*, 1995; Ninan and Arancio, 2004) (Supplementary Materials and methods).

Vesicle cycling

Coverslips with neurons were mounted on a Plexiglas chamber on the stage of a laser scanning confocal microscope. Synaptic vesicles were stained with FM4-64 by perfusing the neurons with bath solution containing 10 μ M FM4-64 and evoking action potentials (Supplementary Materials and methods, Supplementary Figure S6).

Data analysis

Statistical analyses were performed with Student's *t*-test, ANOVA and *post hoc* comparison. Most data were normalized to the basal values and results were expressed as mean \pm standard error mean (s.e.m.). Data on probability measurements are presented as a range with median and analyzed by WPMT.

Supplementary data

Supplementary data are available at *The EMBO Journal* Online (<http://www.embojournal.org>).

Acknowledgements

This work was supported by NIH (NS 40045-49442). We thank Drs Richard Scheller and Yasunori Hayashi for providing the plasmids of VAMP2-GFP and GluR1-GFP, respectively.

References

- Ahmari SE, Buchanan J, Smith SJ (2000) Assembly of presynaptic active zones from cytoplasmic transport packets. *Nat Neurosci* **3**: 445–451
- Allen C, Stevens CF (1994) An evaluation of causes for unreliability of synaptic transmission. *Proc Natl Acad Sci USA* **91**: 10380–10383
- Antonova I, Arancio O, Trillat AC, Wang HG, Zablow L, Udo H, Kandel ER, Hawkins RD (2001) Rapid increase in clusters of presynaptic proteins at onset of long-lasting potentiation. *Science* **294**: 1547–1550
- Arancio O, Kandel ER, Hawkins RD (1995) Activity-dependent long-term enhancement of transmitter release by presynaptic 3',5'-cyclic GMP in cultured hippocampal neurons. *Nature* **376**: 74–80
- Benke TA, Luthi A, Isaac JT, Collingridge GL (1998) Modulation of AMPA receptor unitary conductance by synaptic activity. *Nature* **393**: 793–797
- Bi GQ, Poo MM (1998) Synaptic modifications in cultured hippocampal neurons: dependence on spike timing, synaptic strength, and postsynaptic cell type. *J Neurosci* **18**: 10464–10472

- Buchs PA, Muller D (1996) Induction of long-term potentiation is associated with major ultrastructural changes of activated synapses. *Proc Natl Acad Sci USA* **93**: 8040–8045
- Carroll RC, Lissin DV, von Zastrow M, Nicoll RA, Malenka RC (1999) Rapid redistribution of glutamate receptors contributes to long-term depression in hippocampal cultures. *Nat Neurosci* **2**: 454–460
- Choi S, Klingauf J, Tsien RW (2000) Postfusional regulation of cleft glutamate concentration during LTP at 'silent synapses'. *Nat Neurosci* **3**: 330–336
- Dobrunz LE, Stevens CF (1997) Heterogeneity of release probability, facilitation, and depletion at central synapses. *Neuron* **18**: 995–1008
- East SJ, Garthwaite J (1991) NMDA receptor activation in rat hippocampus induces cyclic GMP formation through the L-arginine-nitric oxide pathway. *Neurosci Lett* **123**: 17–19
- Emptage NJ, Reid CA, Fine A, Bliss TV (2003) Optical quantal analysis reveals a presynaptic component of LTP at hippocampal Schaffer-associational synapses. *Neuron* **38**: 797–804
- Hayashi Y, Shi SH, Esteban JA, Piccini A, Poncer JC, Malinow R (2000) Driving AMPA receptors into synapses by LTP and CaMKII: requirement for GluR1 and PDZ domain interaction. *Science* **287**: 2262–2267
- Hessler NA, Shirke AM, Malinow R (1993) The probability of transmitter release at a mammalian central synapse. *Nature* **366**: 569–572
- Humeau Y, Shaban H, Bissiere S, Luthi A (2003) Presynaptic induction of heterosynaptic associative plasticity in the mammalian brain. *Nature* **426**: 841–845
- Kase H (1988) New inhibitors of protein kinases from microbial source. In *Proceedings of Seventh International Symposium on Biology of Actinomycetes*, Okami Y, Beppu T, Ogawara H (eds) pp 159–164. Tokyo: Japan Scientific Societies Press
- Liao D, Hessler NA, Malinow R (1995) Activation of postsynaptically silent synapses during pairing-induced LTP in CA1 region of hippocampal slice. *Nature* **375**: 400–404
- Lissin DV, Carroll RC, Nicoll RA, Malenka RC, von Zastrow M (1999) Rapid, activation-induced redistribution of ionotropic glutamate receptors in cultured hippocampal neurons. *J Neurosci* **19**: 1263–1272
- Liu G, Choi S, Tsien RW (1999) Variability of neurotransmitter concentration and nonsaturation of postsynaptic AMPA receptors at synapses in hippocampal cultures and slices. *Neuron* **22**: 395–409
- Liu G, Tsien RW (1995) Properties of synaptic transmission at single hippocampal synaptic boutons. *Nature* **375**: 404–408
- Liu S, Ninan I, Antonova I, Battaglia F, Trinchese F, Narasanna A, Kolodilov N, Dauer W, Hawkins RD, Arancio O (2004) alpha-Synuclein produces a long-lasting increase in neurotransmitter release. *EMBO J* **23**: 4506–4516
- Lu W, Man H, Ju W, Trimble WS, MacDonald JF, Wang YT (2001) Activation of synaptic NMDA receptors induces membrane insertion of new AMPA receptors and LTP in cultured hippocampal neurons. *Neuron* **29**: 243–254
- Ma L, Zablow L, Kandel ER, Siegelbaum SA (1999) Cyclic AMP induces functional presynaptic boutons in hippocampal CA3-CA1 neuronal cultures. *Nat Neurosci* **2**: 24–30
- Malgaroli A, Tsien RW (1992) Glutamate-induced long-term potentiation of the frequency of miniature synaptic currents in cultured hippocampal neurons. *Nature* **357**: 134–139
- Matsuzaki M, Honkura N, Ellis-Davies GC, Kasai H (2004) Structural basis of long-term potentiation in single dendritic spines. *Nature* **429**: 761–766
- Murthy VN, Stevens CF (1998) Synaptic vesicles retain their identity through the endocytic cycle. *Nature* **392**: 497–501
- Neuhoff H, Roeper J, Schweizer M (1999) Activity-dependent formation of perforated synapses in cultured hippocampal neurons. *Eur J Neurosci* **11**: 4241–4250
- Ninan I, Arancio O (2004) Presynaptic CaMKII is necessary for synaptic plasticity in cultured hippocampal neurons. *Neuron* **42**: 129–141
- Ninan I, Liu S, Arancio O (2005) Tetanus-induced presynaptic remodeling in cultured hippocampal neurons. *Soc Neurosci Abstracts*, Washington, p 2005 2610.2012
- Palmer MJ, Isaac JT, Collingridge GL (2004) Multiple, developmentally regulated expression mechanisms of long-term potentiation at CA1 synapses. *J Neurosci* **24**: 4903–4911
- Pickard L, Noel J, Duckworth JK, Fitzjohn SM, Henley JM, Collingridge GL, Molnar E (2001) Transient synaptic activation of NMDA receptors leads to the insertion of native AMPA receptors at hippocampal neuronal plasma membranes. *Neuropharmacology* **41**: 700–713
- Reid CA, Dixon DB, Takahashi M, Bliss TV, Fine A (2004) Optical quantal analysis indicates that long-term potentiation at single hippocampal mossy fiber synapses is expressed through increased release probability, recruitment of new release sites, and activation of silent synapses. *J Neurosci* **24**: 3618–3626
- Renger JJ, Egles C, Liu G (2001) A developmental switch in neurotransmitter flux enhances synaptic efficacy by affecting AMPA receptor activation. *Neuron* **29**: 469–484
- Rosenmund C, Clements JD, Westbrook GL (1993) Nonuniform probability of glutamate release at a hippocampal synapse. *Science* **262**: 754–757
- Rosenmund C, Stevens CF (1996) Definition of the readily releasable pool of vesicles at hippocampal synapses. *Neuron* **16**: 1197–1207
- Ryan TA, Ziv NE, Smith SJ (1996) Potentiation of evoked vesicle turnover at individually resolved synaptic boutons. *Neuron* **17**: 125–134
- Sampo B, Kaech S, Kunz S, Banker G (2003) Two distinct mechanisms target membrane proteins to the axonal surface. *Neuron* **37**: 611–624
- Shi SH, Hayashi Y, Petralia RS, Zaman SH, Wenthold RJ, Svoboda K, Malinow R (1999) Rapid spine delivery and redistribution of AMPA receptors after synaptic NMDA receptor activation. *Science* **284**: 1811–1816
- Slutsky I, Sadeghpour S, Li B, Liu G (2004) Enhancement of synaptic plasticity through chronically reduced Ca²⁺ flux during uncorrelated activity. *Neuron* **44**: 835–849
- Stevens CF, Sullivan JM (1998) Regulation of the readily releasable vesicle pool by protein kinase C. *Neuron* **21**: 885–893
- Stewart MG, Medvedev NI, Popov VI, Schoepfer R, Davies HA, Murphy K, Dallerac GM, Kraev IV, Rodriguez JJ (2005) Chemically induced long-term potentiation increases the number of perforated and complex postsynaptic densities but does not alter dendritic spine volume in CA1 of adult mouse hippocampal slices. *Eur J Neurosci* **21**: 3368–3378
- Sumi M, Kiuchi K, Ishikawa T, Ishii A, Hagiwara M, Nagatsu T, Hidaka H (1991) The newly synthesized selective Ca²⁺/calmodulin dependent protein kinase II inhibitor KN-93 reduces dopamine contents in PC12h cells. *Biochem Biophys Res Commun* **181**: 968–975
- Toni N, Buchs PA, Nikonenko I, Bron CR, Muller D (1999) LTP promotes formation of multiple spine synapses between a single axon terminal and a dendrite. *Nature* **402**: 421–425
- Toni N, Buchs PA, Nikonenko I, Povelaitite P, Parisi L, Muller D (2001) Remodeling of synaptic membranes after induction of long-term potentiation. *J Neurosci* **21**: 6245–6251
- Wang HG, Lu FM, Jin I, Udo H, Kandel ER, de Vente J, Walter U, Lohmann SM, Hawkins RD, Antonova I (2005) Presynaptic and postsynaptic roles of NO, cGK, and RhoA in long-lasting potentiation and aggregation of synaptic proteins. *Neuron* **45**: 389–403